# Otoconin-90, the mammalian otoconial matrix protein, contains two domains of homology to secretory phospholipase A$_2$

Yunxia Wang*, Paul E. Kowalski[†], Isolde Thalmann[‡], David M. Ornitz*[§], Dixie L. Mager[†], and Rudiger Thalmann[‡]

Departments of *Molecular Biology and Pharmacology and [‡]Otolaryngology, Washington University Medical School, St. Louis, MO 63110; and [†]Terry Fox Laboratory, British Columbia Cancer Agency, Vancouver, BC Canada V5Z 1L3

*Communicated by Philip Leder, Harvard Medical School, Boston, MA, October 22, 1998 (received for review September 15, 1998)*

**ABSTRACT** The ability to sense orientation relative to gravity requires dense particles, called otoconia, which are localized in the vestibular macular organs. In mammals, otoconia are composed of proteins (otoconins) and calcium carbonate crystals in a calcite lattice. Little is known about the mechanisms that regulate otoconial biosynthesis. To begin to elucidate these mechanisms, we have partially sequenced and cloned the major protein component of murine otoconia, otoconin-90 (OC90). The amino acid sequence identified an orphan chimeric human cDNA. Because of its similarity to secretory phospholipase A$_2$ (sPLA$_2$), this gene was referred to as *PLA$_2$-like (PLA2L)* and enabled the identification of human *Oc90*. Partial murine cDNA and genomic clones were isolated and shown to be specifically expressed in the developing mouse otocyst. The mature mouse OC90 is composed of 453 residues and contains two domains homologous to sPLA$_2$. The cloning of *Oc90* will allow an examination of the role of this protein in otoconial biosynthesis and in diseases that affect the vestibular system.

Sensitivity to gravity is essential for spatial orientation. Consequently, the gravity receptor system is one of the phylogenetically oldest sensory systems, and the special adaptations that enhance sensitivity to gravity are highly conserved. The gravity receptor cells of the macular epithelia do not differ in any significant way from other vertebrate mechanoreceptor cells, which are conserved from the lateral-line organ of the fish to the mammalian vestibular and auditory organs. Specificity to gravity is imparted by the otoconial complex, which contains biomineral particles called otoconia which, by virtue of their high mass, enhance the ability of macular hair cells to respond to gravity. In mammals, ototonia range in size from 0.1 to 25 $\mu$m and consist of a glycoprotein matrix in a mosaic of microcrystals of CaCO$_3$ organized in a calcite lattice (1–4). The inorganic phase is characterized by an evolutionary trend toward deposition of crystal polymorphs of CaCO$_3$ of increasing stability. The least stable polymorph (vaterite) is present in the primitive otoconia of the hagfish, aragonite predominates in amphibia and reptiles, and birds and mammals are characterized by calcite, the most stable polymorph (3–5).

The organic phase of otoconia consists of a single major glycoprotein species (which accounts for >90% of the total protein) and several less abundant proteins (6, 7). Significantly, each crystal polymorph is associated with a unique major otoconial protein (otoconin), suggesting that the otoconins influence the type of crystal polymorph formed (8).

The biological mechanisms responsible for development, biosynthesis, and maintenance of otoconia are not completely understood. The prevailing hypothesis is that otoconia are formed in the extracellular space from the calcium and carbonate ions of endolymph (3, 4, 9). Because of the low concentration of these ions in endolymph, it is believed that matrix proteins are required for the nucleation and growth of the crystals (1, 3, 4). However, to date, the mechanisms regulating otoconial biosynthesis are not known.

The morphological aspects of the development of the mammalian vestibular system have been studied most extensively in the mouse and the rat. In the mouse, morphogenesis of otoconia begins on embryonic day 14 (E14), when the first seeding of calcium crystals can be observed. The rate of calcification is highest on E15 and E16, when otoconia with defined forms can first be observed. The growth of otoconia appears to be essentially complete by the seventh postnatal day (1, 10–14). Although low rates of otoconial calcium turnover are observed in adult rodents (3, 4), very little is known about the turnover of the organic matrix.

The major otoconin of the aragonitic otoconia, otoconin-22 (OC22) of *Xenopus laevis*, has been sequenced (15). It contains 127 amino acid residues and is heavily glycosylated. Interestingly, OC22 is 37% identical to secretory phospholipase A$_2$ (sPLA$_2$); however, the protein has diverged in the calcium-binding and catalytic domains, which are conserved among the sPLA$_2$s.

The only mammalian otoconial protein identified to date is osteopontin. Osteopontin was observed in the peripheral aspects of otoconia by using immunohistochemistry and in the macular epithelia by using *in situ* hybridization (16). Significantly, osteopontin mRNA is present both in embryos and in the adult, suggesting that some turnover of the organic component of otoconia does occur in the adult (16).

Because otoconin-90 (OC90) accounts for >90% of the total otoconial protein (6, 7) its identification and characterization is fundamental to elucidate the mechanism involved in the morphogenesis of otoconia. In the present paper, we obtained a partial amino acid sequence for both mouse and guinea pig OC90. These sequences were found to be homologous to an orphan chimeric human cDNA (transcribed from an endogenous human retroviral long terminal repeat) that has two regions of homology with sPLA$_2$ (17). We subsequently isolated a partial murine cDNA and genomic clone and demonstrated expression in the developing otocyst by using reverse transcription–PCR (RT-PCR).

## MATERIALS AND METHODS

**Tissue Preparation for Biochemical Analysis.** For gel electrophoresis, tissue samples were prepared and run as described

(7, 18). For amino acid sequencing, dissected otoconia were isolated by using three cycles of suspension in 0.1% SDS/0.1 M sodium acetate (pH 7.4), followed by sonication for 3 min and centrifugation at $10,000 \times g$ for 1 min. The otoconial proteins then were extracted with 100 mM EDTA (pH 7.0) for 24 hr at 4°C. The dried samples were used directly for N-terminal amino acid sequencing.

**Genomic Cloning and Sequencing.** A gridded C57BL/6J mouse genomic P1 library was obtained from the Reference Library Database (19) and screened with a mixture of a 383-bp *Pst*I fragment (residues 995–1,378) and a 320-bp *Hin*dIII/*Ava*I fragment (residues 1,665–1,985) from the human PLA2L cDNA (identified as the human homologue to mouse OC90 N-terminal sequence; ref. 17). These fragments span the two domains of homology with PLA₂. Positive P1 clones were isolated, digested with various restriction enzymes, and shotgun-ligated into pBluescript KS (Stratagene). A 5.8-kb *Hin*dIII fragment (308H) was identified by using hybridization (at reduced stringency, 55°C) to the human PLA2L cDNA fragment encoding the region homologous to mouse/guinea pig *Oc90*. By using a mouse genomic probe derived from the 3′ end of 308H (a 651-bp *Acc*I fragment), an overlapping 4.1-kb *Bam*HI fragment was cloned. Both the 5.8-kb and 4.1-kb fragments were sequenced.

**RT-PCR.** Otocysts from six littermate embryos were pooled, and total RNA was extracted by using the RNeasy kit (Qiagen, Chatsworth, CA). Five micrograms of total RNA was reverse-transcribed by using 25 units of avian myoblastosis virus reverse transcriptase (AMV RTase, Boehringer Mannheim) primed with 2.7 $\mu$g of random hexamer (Pharmacia), 0.5 mM dNTPs, and 40 units of RNase inhibitor. After incubation for 10 min at room temperature and reverse transcription for 45 min at 42°C, cDNA products were denatured at 95°C for 5 min, and aliquots were amplified by using PCR. The primers used were Oto1 (5′-CCATGCTCTGGACACACCAAAT-3′) and Oto2 (5′-ACTCGTCCACAGGCATCCCTT-3′) and are diagrammed in Fig. 4. Each 15-$\mu$l PCR mixture consisted of approximately 20 ng of cDNA, 0.4 mM primers, 0.2 mM dNTPs, 0.75 units of *Taq* polymerase (Boehringer Mannheim), and supplied buffer. PCR was carried out with 35 cycles of 45 sec at 95°C, 60 sec at 57°C, and 60 sec at 72°C, with a final one-step extension for 5 min at 72°C (Hybaid thermal cycler, Woodbrige, NJ).

## RESULTS

**Purification and Amino Acid Sequencing of OC90.** Extracted otoconial proteins of guinea pig and mouse were subjected to two-dimensional PAGE (Fig. 1). The major otoconin, estimated to constitute at least 90% of the total
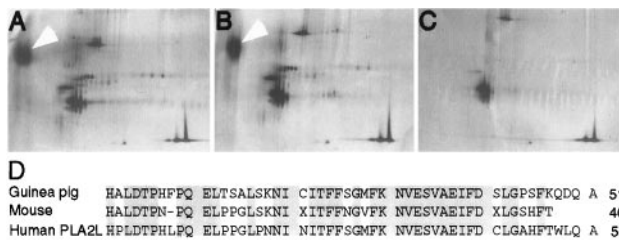


D
| | | | | | |
|---|---|---|---|---|---|
| Guinea pig | HALDTPHFPQ | ELTSALSKNI | CITFFSGMFK | NVESVAEIFD | SLGPSFKQDQ A 51 |
| Mouse | HALDTPN-PQ | ELPPGLSKNI | XITTFNGVFK | NVESVAEIFD | XLGSHFT      46 |
| Human PLA2L | HPLDTPHLPQ | ELPPGLPNNI | NITFFSGMFK | NVESVAEIFD | CLGAHFTWLQ A 51 |

FIG. 1. Identification of mouse and guinea pig OC90. Two-dimensional SDS/PAGE separation of proteins (10 $\mu$g dry weight) from isolated otoconia of the mouse (*A*) and guinea pig (*B*). Isoelectric focusing was used in the first dimension (left to right) and SDS/PAGE was used in the second dimension (top to bottom). Protein standards (carbonic anhydrase, ovalbumin, and $\beta$-galactosidase) were run alone (*C*) and spiked into the otoconial preparations shown in *A* and *B*. Arrows identify OC90. (*D*) N-terminal sequence of partially purified mouse and guinea pig otoconins were aligned and used to identify an orphan human cDNA, PLA2L.

protein, appeared as a broad smear at a pI centered at 2.9 and with a molecular mass of $\approx$83 kDa. This band corresponds to the major matrix protein reported by Pote and Ross (6) in the rat and is accordingly referred to as OC90. Four minor bands, all in the acidic region, ranging in molecular mass from 50 to 62 kDa, also were observed but have not yet been identified.

To identify the major otoconial protein of guinea pig and mouse, N-terminal amino acid sequencing was carried out directly on aliquots of protein extract from purified and decalcified otoconia. Forty-six mouse and fifty-one guinea pig N-terminal residues were determined (Fig. 1*D*) and found to be $\approx$75% identical. A BLAST search of protein and nucleic acid databases identified a human cDNA that was $\approx$80% identical to either the mouse or the guinea pig sequence (Fig. 1*D*). The identified human cDNA encoded a novel fusion transcript with two domains of similarity to *sPLA*₂, termed *PLA2L* (17, 20). The only known source of human *PLA2L* mRNA is as part of a chimeric message transcribed from an endogenous retroviral long terminal repeat promoter in teratocarcinoma cells. Expression of *PLA2L* was not detectable in poly(A)⁺ RNA blots of a panel of human tissues and cell lines (17).

**cDNA Sequence of Mouse *Oc90*.** The mouse *Oc90* cDNA sequence (GenBank accession no. AF091846) was assembled by identifying two murine E13.5–E14.5 embryo expressed sequence tag (EST) clones (accession nos. W50767 and AA034721) that were 77% and 69% identical to regions of human *PLA2L*. The two murine EST sequences overlapped by 28 bp and totaled 818 bp. Sequence continuity was confirmed by using PCR amplification and restriction-enzyme analysis. The 3′ end of the murine EST clone corresponding to W50767 was partially sequenced and found to contain the EST AA437511 sequence (Fig. 2). ESTs AA034721 and W50767 encode partial regions of homology to sPLA₂. EST W50767 also contains a translation stop codon and a short poly(A) tail (Fig. 2).

To assemble the 5′ end of the mouse *Oc90* cDNA, mouse genomic clones were isolated and sequenced (see below), and PCR primers were designed based on predicted exon sequence. Oto-1 corresponds to the first 22 bp of exon 1 in mouse genomic DNA (see below), which encodes the N-terminal sequence of OC90. Oto-2 is complementary to the 5′ end of EST AA034721 and is located in genomic exon three. The RT-PCR amplification product from E15.5 mouse head mRNA yielded a 287-bp fragment that corresponded precisely with genomic exon sequence (see below). This sequence and the EST contig, together, encodes a 1,608-bp sequence [excluding the poly(A) tail] that contains a 453-aa ORF but lacks sequence encoding a signal peptide and potential 5′ untranslated mRNA.

The deduced amino acid sequence of the mature OC90 protein (Fig. 3) has a calculated molecular mass of 49 kDa and pI of 4.4. This compares with an apparent molecular mass of 83 kDa and a pI of 2.9 based on electrophoretic behavior.



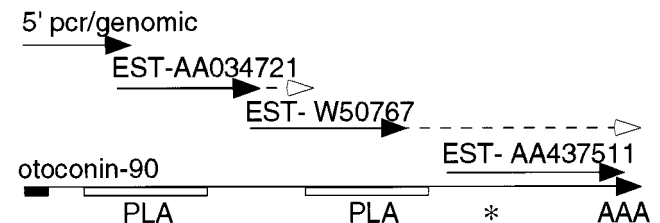FIG. 2. cDNA assembly and structure of mouse *Oc90*. Diagram showing the strategy used to assemble the *Oc90* cDNA. Solid lines show sequences obtained by using PCR amplification or from ESTs. Additional sequencing to extend EST sequences is indicated by dashed lines. Solid box, the region corresponding to N-terminal OC90 sequence; open boxes, the two domains of homology to sPLA₂; *, translation stop codon; AAA, poly(A) tail.
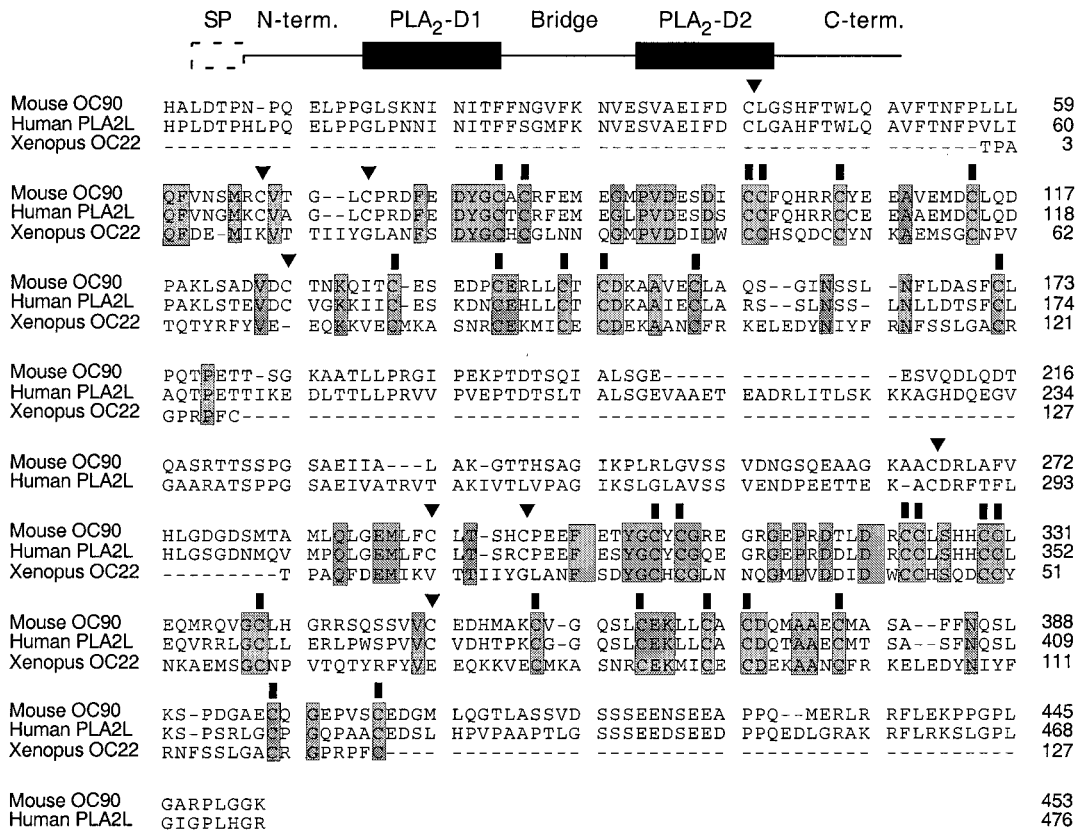
                    SP  N-term.    PLA₂-D1    Bridge    PLA₂-D2    C-term.

```
Mouse OC90    HALDTPN-PQ ELPPGLSKNI NITFFNGVFK NVESVAEIFD CLGSHFTWLQ AVFTNFPLLL   59
Human PLA2L   HPLDTPHLPQ ELPPGLPNNI NITFFSGMFK NVESVAEIFD CLGAHFTWLQ AVFTNFPVLI   60
Xenopus OC22  ---------- ---------- ---------- ---------- ---------- -------TPA    3

Mouse OC90    QFVNSMRCVT G--LCPRDFE DYGCACRFEM EGMPVDESDI CCFQHRRCYE EAVEMDCLQD  117
Human PLA2L   QFVNGMKCVA G--LCPRDFE DYGCTCRFEM EGLPVDESDS CCFQHRRCCE EAAEMDCLQD  118
Xenopus OC22  QFDE-MIKVT TIIYGLANFS DYGCHCGLNN QGMPVDDIDW CQHSQDCYN  KAEMSGCNPV   62

Mouse OC90    PAKLSADVDC TNKQITC-ES EDPCERLLCT CDKAAVECLA QS--GINSSL -NFLDASFCL  173
Human PLA2L   PAKLSTEVDC VGKKIIC-ES KDNCEHLLCT CDKAAIECLA RS--SLNSS- LALLDTSFCL  174
Xenopus OC22  TQTYRFYVE- EQKKVEQMKA SNRCEKMICE CDEKAANCFR KELEDYNIYF RNFSSLGACR  121

Mouse OC90    PQTPETT-SG KAATLLPRGI PEKPTDTSQI ALSGE----- ---------- -ESVQDLQDT  216
Human PLA2L   AQTPETTIKE DLTTLLPRVV PVEPTDTSLT ALSGEVAAET EADRLITLSK KKAGHDQEGV  234
Xenopus OC22  GPREFC---- ---------- ---------- ---------- ---------- ----------  127

Mouse OC90    QASRTTSSPG SAEIIA---L AK-GTTHSAG IKPLRLGVSS VDNGSQEAAG KAACDRLAFV  272
Human PLA2L   GAARATSPPG SAEIVATRVT AKIVTLVPAG IKSLGLAVSS VENDPEETTE K-ACDRFTFL  293

Mouse OC90    HLGDGDSMTA MLQLGEMLFC LT-SHCPEEF ETYGCYCGRE GRGEPRDTLD RCCLSHHCCL  331
Human PLA2L   HLGSGDNMQV MPQLGEMLFC LT-SRCPEEF ESYGCYCGQE GRGEPRDDLD RCCLSHHCCL  352
Xenopus OC22  ---------T PAQFDEMIKV TIIYGLANF  SDYGCHCGLN NQGMPVDID  WCCHSQDCCY   51

Mouse OC90    EQMRQVGCLH GRRSQSSVVC EDHMAKCV-G QSLCEKLLCA CDQMAAECMA SA--FFNQSL  388
Human PLA2L   EQVRRLGCLL ERLPWSPVVC VDHTPKCG-G QSLCEKLLCA CDQTAAECMT SA--SFNQSL  409
Xenopus OC22  NKAEMSGCNP VTQTYRFYVE EQKKVEQMKA SNRCEKMICE CDEKAANCFR KELEDYNIYF  111

Mouse OC90    KS-PDGAEQQ GEPVSQEDGM LQGTLASSVD SSSEENSEEA PPQ--MERLR RFLEKPPGPL  445
Human PLA2L   KS-PSRLGQP GQPAACEDSL HPVPAAPTLG SSSEEDSEED PPQEDLGRAK RFLRKSLGPL  468
Xenopus OC22  RNFSSLGACR GPRPFC---- ---------- ---------- ---------- ----------  127

Mouse OC90    GARPLGGK  453
Human PLA2L   GIGPLHGR  476
```

FIG. 3.  Primary structure and sequence alignment of mouse *Oc90* and *PLA2L* (human OC90) with *Xenopus laevis* OC22. (*Upper*) line diagram of the OC90 ORF. SP, putative signal peptide; N-term., leader domain; PLA₂-D1 and PLA₂-D2, regions of homology to PLA₂ domains; bridge, region linking the two PLA₂ domains; C-term, carboxyl-terminal domain. (*Lower*) sequence alignment between mouse and human OC90 and *Xenopus laevis* OC22 showing alignment of OC22 with both PLA₂ domains of OC90. Residues conserved between all three sequences are shaded. Conserved cysteine residues are marked with a solid bar. Cysteine residues present in mammalian OC90 but not amphibian OC22 are marked with an arrowhead.

OC90 consists of five domains and a putative signal peptide. Most characteristic are two domains homologous to sPLA₂ that exhibit 25–34% amino acid identity with group I and group II sPLA₂ proteins. The PLA domains are joined by a linker domain and are flanked by an N-terminal leader and a C-terminal tail segment (Fig. 3). These sequence segments are not homologous to any known protein.

**Identification of the Mouse *Oc90* Genomic Locus.** To facilitate the identification of the 5′ end of the mouse *Oc90* cDNA, exon sequences were identified in cloned-mouse genomic DNA. A C57BL/6J mouse genomic P1 library was screened with probes (383-*Pst*I and 320-*Hin*dIII/*Ava*I; see *Materials and Methods*) derived from the human PLA2L cDNA. Two P1 clones were identified, digested with *Bam*HI and *Hin*dIII, and shotgun-subcloned into pBluescript KS. Sequencing of a 5.8-kb *Hin*dIII fragment identified an exon encoding the mouse OC90 N-terminal peptide sequence, confirming that a partial genomic clone had been identified. An overlapping 4.1-kb *Bam*HI fragment also was sequenced. Three exons encoding the mouse otoconin N-terminal region were identified within the 8.2 kb of genomic sequence by homology to human PLA2L and by using the GRAIL algorithm to predict coding sequence (21) (Fig. 4). The third identified exon corresponded to sequence at the 5′ end of EST AA034721. As described above, RT-PCR amplification, using primers corresponding to sequence within exons 1 and 3, confirmed the continuity of these three exons and the 5′ end of the murine *Oc90* cDNA.

**Expression of Mouse *Oc90*.** OC90 was not detectable by two-dimensional SDS/PAGE in adult macular epithelia (7). The protein could have been secreted as a precursor, synthesized in perimacular epithelia, or synthesized only during embryonic development. In the present study, *Oc90* mRNA expression therefore was assayed during embryonic development by using RT-PCR. PCR primers were designed to amplify a 287-bp cDNA fragment that spans two introns of genomic DNA (Fig. 4). RT-PCR amplification of E17.5-embryo RNA detected robust expression of *Oc90* mRNA in the otocyst but
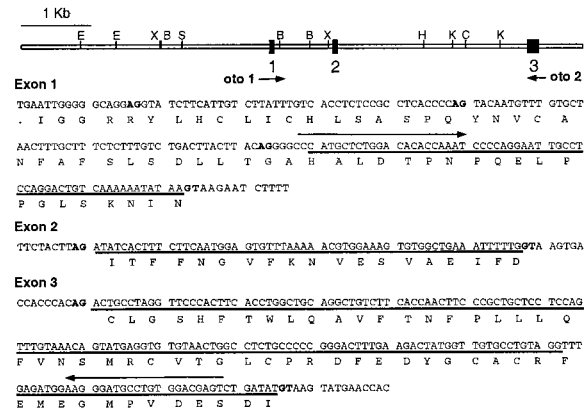
```
 1 Kb
        E E     X B S        B  B X      H  K C   K
 ══════════════════════════════════════════════════
 Exon 1                 1        2              3
                    oto 1 ──►              ◄── oto 2

TGAATTGGGG GCAGGAGGTA TCTTCATTGT CTTATTTGTC ACCTCTCCGC CTCACCCCAG TACAATGTTT GTGCT
.  I  G  G   R  R  Y  L  H  C   L  I  C  H   L  S  A   S  P  Q   Y  N  V  C   A

AACTTTGCTT TCTCTTTGTC TGACTTACTT ACAGGGGCCC ATGCTGTGGA CACACCAAAT CCCCAGGAAT TGCCT
N  F  A  F   S  L  S   D  L  L   T  G  A  H   A  L  D   T  P  N   P  Q  E  L   F

CCAGGACTGT CAAAAAATAT AAGTAAGAAT CTTTT
P  G  L  S   K  N  I  N

Exon 2
TTCTACTTAG ATATCACTTT CTTCAATGGA GTGTTTAAAA ACGTGGAAAG TGTGGCTGAA ATTTTTGGTA AGTGA
           I  T  F   F  N  G   V  F  K  N   V  E  S   V  A  E   I  F  D

Exon 3
CCACCCACAG ACTGCCTAGG TTCCCACTTC ACCTGGCTGC AGGCTGTCTT CACCAACTTC CCGCTGCTCC TCCAG
           C  L  G   S  H  F   T  W  L  Q   A  V  F   T  N  F   P  L  L  L   Q

TTTGTAAACA GTATGAGGTG TGTAACTGGC CTCTGCCCCC GGGACTTTGA AGACTATGGT TGTGCCTGTA GGTTT
F  V  N  S   M  R  C   V  T  G   L  C  P  R   D  F  E   D  Y  G   C  A  C  R   F

GAGATGGAAG GGATGCCTGT GGACGAGTCT GATATGTAAG TATGAACCAC
E  M  E  G   M  P  V   D  E  S   D  I
```

FIG. 4.  Partial genomic structure of *Oc90*. (*Upper*) Restriction map of the cloned 8.1-kb genomic locus showing the location of three coding exons (solid boxes). Arrows indicate the primers (oto 1 and oto 2) used for RT-PCR amplification of the 5′ *Oc90* cDNA. (*Lower*) sequence of exons 1–3 and flanking intron sequence. Potential splice donor (GT) and splice acceptor (AG) nucleotides are shown in bold. ORFs are indicated with single-letter amino acid notation and those encoding *Oc90* are indicated by a solid line. B, *Bam*HI; C, *Cla*I; E, *Eco*RI; H, *Hin*dIII; K, *Kpn*I; S, *Sfi*I; X, *Xba*I.
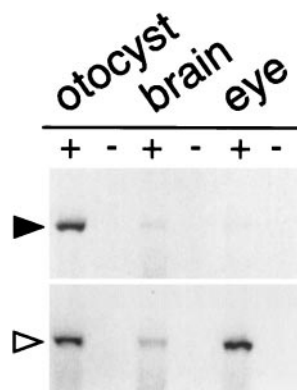
FIG. 5.    Expression of *Oc90* in E17.5 mouse embryo otocysts, brain (minus otocysts), and eyes. Total RNA (5 µg) was reverse-transcribed *in vitro*. cDNA was amplified by using primers Oto1 and Oto2 (marked by arrows in Fig. 4, *Upper*) or by using primers specific for the β-actin cDNA as the positive control (*Lower*). +, with RTase; −, without RTase.

a weak signal in the brain (minus otocyst) and eye (Fig. 5). PCR data were confirmed by using *in situ* hybridization. In contrast to prevailing concepts about the secretion of otoconial matrix proteins (1, 14), *Oc90* mRNA is not expressed in the macular sensory epithelia but was observed in nonsensory epithelia of both the vestibular and cochlear portions of the developing inner ear (unpublished results).

## DISCUSSION

To begin to understand molecular mechanisms involved in mammalian vestibular development, we have cloned the gene encoding the predominant protein of otoconia, OC90. OC90 was isolated from mouse and guinea pig otoconia, and the N termini were sequenced by using Edman degradation. Database searching identified an orphan human homologue related to sPLA$_2$ called PLA2L. This human cDNA was, in turn, used to identify overlapping murine ESTs and genomic clones, which, along with RT-PCR, were used to assemble the *Oc90* cDNA. RT-PCR was used to identify *Oc90* expression in the developing otocyst.

Determination of the N-terminal sequence of native *Oc90* not only allowed derivation of the entire murine sequence but also defined the N terminus of the corresponding mature human homolog. Mature OC90 does not start with a methionine, and the first residue (His) likely represents the cleavage position of the mature protein from a signal peptide-containing precursor. An in-frame methionine lies 17 aa upstream of the OC90 ORF within the HERV-H-PLA2L sequence (17, 20). This sequence is likely to encode a signal sequence as predicted by using the SIGNALP and SIGSCAN search algorithms (22, 23). Preliminary data by using rapid amplification of cDNA ends to identify additional 5′ sequence in the mouse also identified a potential signal sequence with homology to the human sequence (P.E.K., unpublished observation).

Numerous lines of evidence indicate that otoconia are synthesized primarily during embryonic development, with the rate of synthesis peaking in the mouse on E16 and otoconial calcification essentially completed by several days postpartum (1, 9, 12–14). *Oc90* mRNA was first identified in the otocyst on E12.5 (which predates the appearance of otoconia by 1–2 days), with maximum expression observed on E16.5 (Y.W., unpublished data). Significantly, OC90 protein is detectable neither in macular epithelia—the presumed site of synthesis and secretion of otoconial proteins—nor in the gelatinous membrane of adult animals (7). It is possible that in the adult, the only source of OC90 protein is that which is sequestered

within the otoconial CaCO$_3$ shell, essentially in a fossilized state. In retrospect, attempts to identify the physiological site of human PLA2L expression was unsuccessful (17) before acquisition of the N-terminal sequence from murine tissue-derived OC90 because of the very restricted spatial and temporal expression of *Oc90* mRNA.

Human PLA2L/OC90 is only 27% identical with amphibian OC22, and this degree of homology is low enough and spread over a wide enough region that it was not revealed by using database searching (17, 20). Kowalski *et al.* (20) have determined that the insertion of the retroviral *HERV-H* element into the *PLA2L* locus occurred approximately 15–20 million years ago, is limited to the genome of higher primates, and does not affect other mammals (including the mouse). Alternate splicing from the *HERV-H* element yields a *HERV-H-PLA2L* fusion transcript that is expressed in some teratocarcinoma cell lines. The complete coding sequence and expression of the endogenous human *PLA2L* gene is not known.

The difference between the calculated and apparent molecular mass of murine OC90 is primarily the result of nonhomogeneous glycosylation, which is apparent from the multiple size and charge variants seen on SDS gels (Fig. 1) and from a shift in migration after deglycosylation (I.T., unpublished data). Moreover, the amphibian OC22 homologue is heavily glycosylated (15), and overexpressed human PLA2L appears glycosylated (24). Indirect evidence suggests that glycosaminoglycans account for much of the posttranslational modifications of OC90 (I.T., unpublished data).

The most characteristic feature of the PLA domains of OC90 is the large number of cysteine residues corresponding to the conserved disulfide bonds, which are a hallmark of the sPLA$_2$ structure (25–28). These disulfide bonds are responsible for the exceptionally rigid structure of sPLA$_2$, which is essential for the prolonged maintenance of catalytic activity in an unfavorable extracellular environment. The location of conserved disulfide bridges form the basis for the traditional classification scheme for sPLAs into types I and II (26). The classical sPLA$_2$ types I and II consist of seven disulfide bonds, of which six are shared, whereas the seventh disulfide bond is specific to and characteristic of each type. The seven disulfide bonds of the N-terminal PLA domain 1 of OC90 are characteristic of type I. However, the C-terminal domain 2 contains eight disulfide bonds (including both type-specific bonds), an arrangement not known to exist at the time when the classical typing scheme was designed (26, 29). Recently, a catalytically active mammalian sPLA$_2$ containing the eight disulfide bonds was discovered and named sPLA$_2$ type X (30) in accordance with the updated classification scheme (27). In addition, both domains contain an unmatched cysteine residue in the same conserved position (C-16, Fig. 6), which conceivably participates in the formation of an interdomain disulfide bond. The unmatched cysteine residue in equivalent positions of the N-terminal and bridge regions (17 and 16 residues upstream from the start of the respective PLA2 domains; Fig. 3) likewise may serve as structural reinforcements.

In summary, it is evident that the PLA domains of OC90 exhibit an unprecedented combination of structural features hitherto considered specific for either one or the other of the canonical types of sPLA$_2$s. This would place OC90 ancestral to the emergence of type I and II sPLA$_2$s before the divergence of mammals from reptiles as postulated by Pote *et al.* (15) for amphibian OC22. In fact, phylogenetic analysis places both PLA domains of OC90, amphibian OC22, and sPLA$_2$ type X on the same branch ancestral to other contemporarily expressed reptilian or mammalian sPLA$_2$s (R.T., unpublished observation). Only the honeybee venom PLA is more distantly related (17, 20).

Alignment of OC90 domains with several representative sPLA$_2$ homologues indicates a highly conserved region (≈40 residues) close to the N terminus (Fig. 6). Levels of identity

```
                                      C11    C16         Y28 G30 G32              H48 C50
                                       |      |           |  |  |                 |  ||
Xenopus OC22                  TPAQFDEMI- KVTTIIYGLA NFSDYGCHCG LNNQGMPVDD IDWCCHSQDC   49
Mouse OC90 domain 1           LLLQFVNSMR CVTG--LCPR DFEDYGCACR FEMEGMPVDE SDICCFQHRR  105
Mouse OC90 domain 2           AMLQLGEMLF CLT--SHCPE EFETYGCYCG REGRGPRDT LDRCCLSHHC  330
Human pancreatic PLA2 (group I)  K------MIK CVIPGSDPFL EYNNYGCYCG LGGSGTPVDK LDKCCQTHDN   73
Human synovial PLA2 (group II)   NLVNFHRMI- KLTTGKEAAL SYGFYGCHCG VGGRGSPKEA TDRCCVTHDC   70
Mouse testicular PLA2 (group IIC) SSFWQFQRMV KHVTGRSAFF SXYGYGCYCG LGGKGLPVDA TDRCCWAHDC   70
Rat testicular PLA2 (Group V)    GLLDLKSMIE KVTGKNALT- NYGFYGCYCG WGGRGTPKDG TDWCCWAHDH   70
Human fetal lung PLA2 (group X)  GILELAGTVG CVGP--RTPI AYMKYGCFCG LGGHGQPRDA IDWCCHGHDC   91
β bungarotoxin                   NLINFMEMIR YTIPCEKTWG EYADYGCYCG AGGSGRPIDA LDRCCVHDC    50
Caudoxin (group II)              NLIQFGNMIS AMTG--KSSL AYASYGCYCG WGGKGQPKDD TDRCCFVHDC   48
Myotoxin (group I)               NLVQFSYVIT CANHNRRSSL DYADYGCYCG AGGSGTPVDE LDRCCKIHDD   50
                                                       Ca2+ loop    active site
```

```
                                 Y52              Y73 C77                    D99
                                  |                |  |                       |
Xenopus OC22                  CYNKAEMS-G CNPVT--QTY RFY-VEE-QK KVECMKASNR -CEKMICECD   93
Mouse OC90 domain 1           CYEEAVEM-D CLQD---PAK LSADVDCTNK QITCESEDP- -CERLLCTCD  149
Mouse OC90 domain 2           CLEQMRQV-G CLHG----RR SQSSVVCEDH MAKCVGQSL- -CEKLLCACD  373
Human pancreatic PLA2 (group I)  CYDQAKKLDS CKFLLDNPYT HTYSYSCSGS AITCSSK-NK ECEAFICNCD  122
Human synovial PLA2 (group II)   CYKRLEKR-G CGTK-----F LSYKFSNSGS RITC-AKQDS -CRSQLCECD  112
Mouse testicular PLA2 (group IIC) CYHKLKEY-G CQPILNA--- YQFTIVNGTV TCGSTVASSC PCGQKACECD  126
Rat testicular PLA2 (Group V)    CYGRLEEK-G CNIRT----- QSYKYRFAWG VVTC--EPGP FCHVNLCACD  112
Human fetal lung PLA2 (group X)  CYTRAEEA-G CSPKT----- ERYSWQCVNQ SVLCGPAENK -CQELLCKCD  134
β bungarotoxin                   CYGDAEKKHK CNPKT----- SQYSYKLTKR TIIC-YGAAG TCGRIVCDCD   94
Caudoxin (group II)              CYGKADK--- CSPKM----- ILYSYKFHNG NIVC--GDKN ACKKKVCECD   88
Myotoxin (group I)               CYGEAEKQ-G CYPKM----- LMYDYYCGSN GPYC-RNVKK KCNRKVCDCD   93
                                 pancreatic loop
```

```
                                                       C133
                                                        |
Xenopus OC22                  EKAANCFRKE LEDYNIYFRN F-SSLGACRG PRPFC-   127
Mouse OC90 domain 1           KAAVECLAQS --GINSSLNF L-DASF-CLP QTPET-   174
Mouse OC90 domain 2           QMAAECMASA --FFNQSLKS --PDGAECQG EPVSC-   404
Human pancreatic PLA2 (group I)  RNAAICFSKA --PYNKAHKN L-DTKKYCQS ------   149
Human synovial PLA2 (group II)   KAAATCFARN KTTYNKKYQY Y--SNKHCRG STPRC-   145
Mouse testicular PLA2 (group IIC) KQSVYCRKEN LATYEKAFKQ LFPTRPQCGR DKLQC-   151
Rat testicular PLA2 (Group V)    RKLVYCLKRN LRSYNPQ-YQ YFP-NILCS- ------   139
Human fetal lung PLA2 (group X)  QEIANCLAQT --EYNLKYLF Y-PQF-LCEP DSPKCD   166
β bungarotoxin                   RTAALCFGQS --DYIEGHKN I-DTARFCQ- ------   120
Caudoxin (group II)              RVAAICFAAS KHSYNKNLWR Y-PSSK-CTG TAEKC-   121
Myotoxin (group I)               VAAAELFARN --AYNNANYN I-DTKKRCK- ------   119
```
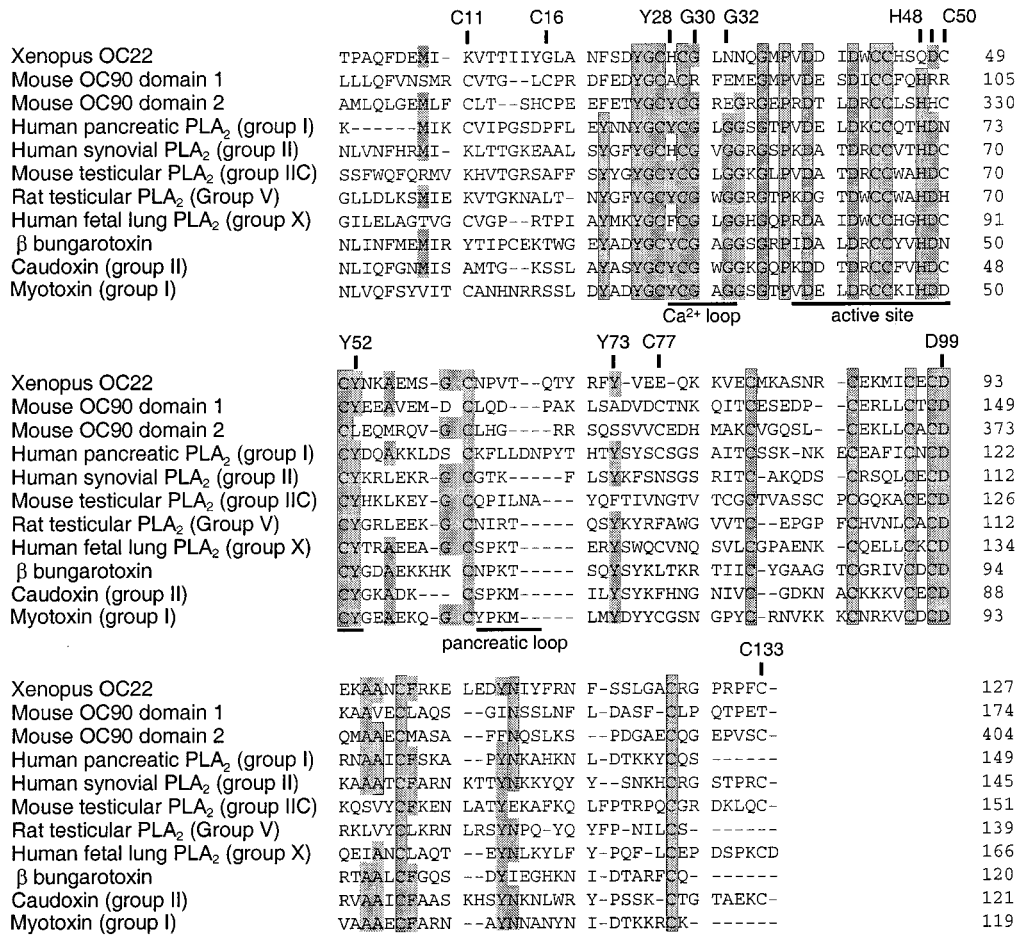
FIG. 6.    Alignment of the PLA2-like domains of mouse OC90 and *Xenopus lavius* OC22 with sPLA2s. Alignments of the indicated amino acid sequences were made by using GENE WORKS software and refined manually. Shaded residues are present in at least 7 of the 11 sequences shown. These sequences represent the mammalian sPLA2 Groups IA (human pancreatic PLA2; ref. 37), IIA (human synovial PLA2; ref. 38), IIC (mouse testicular PLA2; ref. 39), V (rat testicular PLA2; ref. 40) and X (human fetal lung PLA2; ref. 30), and the snake venom PLA2s, caudoxin (group II; ref. 41), myotoxin (group I; ref. 42), and β1 bungarotoxin A1 (43).The calcium-binding loop, catalytic site, and pancreatic loop (29, 30, 44, 45) are underlined. Labeled residues are numbered as in ref. 29.

with other homologues within the conserved regions are as high as 50%. The conserved N-terminal region includes both the essential calcium-binding loop and the catalytically active site. However, some of the residues considered essential for calcium binding (Y28, G30, G32, D49 in Fig. 6; refs. 26 and 29) and for catalytic activity (H48, Y52, Y73, D99 in Fig. 6; ref. 29) are replaced in both PLA2 domains of OC90. It is therefore likely that neither the calcium-binding loop nor the catalytic site are functional. In a detailed structural analysis of the amphibian homologue OC22 (which lacks H48), Pote *et al.* (15) had arrived at the same conclusion corroborated by using biochemical studies. However, it is likely that the capacity to bind phospholipid substrates is conserved.

An important feature of both PLA domains is the very acidic pIs (3.9 and 4.9 for PLA domains 1 and 2, respectively). PLA domain 1 contains 22 acidic residues, and PLA domain 2 contains 17 acidic residues. These observations characterize the PLA domains of OC90 as the most acidic sPLA homologues, only approached in degree of acidity by OC22 and sPLA2 type X (30). In the case of the otoconins, the acidic residues likely represent a specific adaptation for the binding of $Ca^{2+}$ ions (see below).

Intriguingly, as suggested by Pote and Ross (8), the calcitic otoconia of the amphibian utricle may contain the same matrix protein as mammalian otoconia, namely OC90. This would mean that the genome of amphibia contains genes encoding both the aragonitic OC22 from the saccule and the calcitic

OC90 from the utricle. If confirmed, this would allow a rigorous examination of the evolutionary relationship between the two classes of otoconial proteins and would enable a comparison with the catalytically active homologues in the amphibian genome.

To explain the role of OC22 in the determination of aragonitic otoconia, Pote *et al.* (15) compared the crystal structure of *Crotalis atrox* venom (a type II PLA2 homologue) with a computer simulation of the three-dimensional structure of OC22 and found the two structures virtually superimposable. However, because neither the calcium-binding loop nor the catalytically active site of OC22 appeared functional, it was concluded that OC22 is limited to a structural role usurped from sPLA2 because of the unusual rigidity of this molecule, a feature that should also make it ideally suited to serve as the scaffold for a crystal lattice. Future studies should attempt to determine the precise location of the acidic residues at the surface of the PLA domains and to identify carboxylate groups in favorable positions to bind the calcium ions of the crystal lattice.

If the structure of OC22 is specifically adapted to serve as a scaffold for the aragonite lattice, it follows that OC90 should specify a calcitic lattice. However, the presence of two PLA domains in the same molecule is a complicating feature in the latter instance and suggests that the dimeric structure is particularly suited to fit the geometry of the calcite lattice. The pronounced divergence of the two domains [not only in terms

of disulfide bonds but also in the number and species of acidic residues (Fig. 6)] and in the values of the calculated pIs support this hypothesis. Alternatively, the second domain may represent merely an additional unit, with both domains performing identical roles in crystal nucleation and growth, despite their divergence.

Other interacting factors, including the less abundant otoconins (all of which are acidic) and constituents of the gelatinous phase of the otoconial complex, will contribute to the formation and maintenance of otoconia. Of special significance is the globular substance, which consists of membrane-bound vesicles trapped within the gelatinous phase of the otoconial complex and generally is considered the precursor of otoconia (31). These particles are likely the extracellular counterparts of calcium-enriched secretory granules recently identified in the cytoplasm of macular supporting cells (32). We propose that a key event in the formation of otoconia requires an interaction between OC90 and the globular substance. In this hypothetical model, the organized layer of acidic phospholipids of the globular substance leads to a high localized concentration of calcium. On binding of OC90 to the lipid layer, the concomitant conformational change may facilitate stabilization of calcium at binding sites within the PLA domains of OC90, with subsequent incorporation into the growing calcite lattice. The glycosaminoglycan portion of OC90 may act in the controlled inhibition of crystal growth. This model also explains the exclusive localization of otoconia to the macular superstructure, even though *Oc90* is expressed throughout the entire developing inner ear (a more detailed account is presented in ref. 33).

Well characterized mouse mutants with defects in the vestibular system have been described, although none of them map genetically to the *Oc90* locus on chromosome 15 (data not shown). The *tilted-head, tilted*, and *head-tilt* mutations, which specifically lack otoconia but appear to have a normal sensory epithelium, map to mouse Chromosomes 1, 5, and 17, respectively (refs. 34–36; D.M.O., unpublished data). It should be noted that the critical defect in otoconial agenesis mutants may lie within the glycosaminoglycan component of OC90 or with its interaction with components of the globular substance. These mutants should provide a genetic means to identify and clone additional structural or regulatory genes that are essential for otoconial development.

1. Lim, D. J. (1980) *Birth Defects* **16,** 111–146.
2. Mann, S., Parker, S. B., Ross, M. D., Skarnulis, A. J. & Williams, R. J. (1983) *Proc. R. Soc. London B* **218,** 415–424.
3. Ross, M. D., Pote, K. G. & Perini, F. (1985) in *Auditory Biochemistry*, ed. Drescher, D. G. (Thomas, Springfield, IL), pp. 500–514.
4. Ross, M. D. & Pote, K. G. (1984) *Philos. Trans. R. Soc. London B* **304,** 445–452.
5. Carlstrom, D. (1963) *Biol. Bull. (Woods Hole, Mass.)* **125,** 441–463.
6. Pote, K. G. & Ross, M. D. (1986) *J. Ultrastruct. Mol. Struct. Res.* **95,** 61–70.
7. Ornitz, D. M., Bohne, B. A., Thalmann, I., Harding, G. W. & Thalmann, R. (1998) *Hearing Res.* **122,** 60–70.
8. Pote, K. G. & Ross, M. D. (1991) *Comp. Biochem. Physiol. B Biochem. Mol. Biol.* **98,** 287–295.
9. Erway, L. C., Purichia, N., Netzler, R., D'Amore, M., Esses, D. & Levine, M. (1986) *Scanning Electron Microsc.* **4,** 1681–1694.
10. Rugh, R. (1990) *The Mouse: Its Reproduction and Development* (Oxford Univ. Press, New York).
11. Anniko, M. (1990) *Development of the Vestibular System* (Wiley, New York).
12. Salamat, M. S., Ross, M. D. & Peacor, D. R. (1980) *Ann. Otol. Rhinol. Laryngol.* **89,** 229–238.
13. Anniko, M. (1980) *Am. J. Otolaryngol.* **1,** 400–410.
14. Veenhof, V. B. (1969) *The Development of Otoconia in Mice* (North–Holland, Amsterdam).
15. Pote, K. G., Hauer, C. R., Michel, H., Shabanowitz, J., Hunt, D. F. & Kretsinger, R. H. (1993) *Biochemistry* **32,** 5017–5024.
16. Takemura, T., Sakagami, M., Nakase, T., Kubo, T., Kitamura, Y. & Nomura, S. (1994) *Hearing Res.* **79,** 99–104.
17. Feuchter-Murthy, A. E., Freeman, J. D. & Mager, D. L. (1993) *Nucleic Acids Res.* **21,** 135–143.
18. Thalmann, R. (1976) in *The Handbook of Auditory and Vestibular Research Methods*, eds. Smith, C. A. & Vernon, J. A. (Thomas, Springfield, IL), pp. 359–419.
19. Zehetner, G. & Lehrach, H. (1994) *Nature (London)* **367,** 489–491.
20. Kowalski, P. E., Freeman, J. D., Nelson, D. T. & Mager, D. L. (1997) *Genomics* **39,** 38–46.
21. Uberbacher, E. C. & Mural, R. J. (1991) *Proc. Natl. Acad. Sci. USA* **88,** 11261–11265.
22. Prestridge, D. S. (1991) *Comput. Appl. Biosci.* **7,** 203–206.
23. Nielsen, H., Engelbrecht, J., Brunak, S. & von Heijne, G. (1997) *Protein Eng.* **10,** 1–6.
24. Kowalski, P. E. & Mager, D. L. (1998) *J. Virol.* **72,** 6164–6168.
25. Zhu, H., Dupureur, C. M., Zhang, X. & Tsai, M. D. (1995) *Biochemistry* **34,** 15307–15314.
26. Davidson, F. F. & Dennis, E. A. (1990) *J. Mol. Evol.* **31,** 228–238.
27. Dennis, E. A. (1997) *Trends Biochem. Sci.* **22,** 1–2.
28. Dennis, E. A. (1994) *J. Biol. Chem.* **269,** 13057–13060.
29. Renetseder, R., Brunie, S., Dijkstra, B. W., Drenth, J. & Sigler, P. B. (1985) *J. Biol. Chem.* **260,** 11627–11634.
30. Cupillard, L., Koumanov, K., Mattei, M. G., Lazdunski, M. & Lambeau, G. (1997) *J. Biol. Chem.* **272,** 15745–15752.
31. Suzuki, H., Ikeda, K. & Takasaka, T. (1995) *Hearing Res.* **90,** 212–218.
32. Harada, Y., Kasuga, S. & Mori, N. (1998) *Acta Otolaryngol. (Stockh.)* **118,** 74–79.
33. Thalmann, R., Echols, R., Wang, Y., Thalmann, I. & Ornitz, D. M. (1999) in *Equilibrium in Research and Equilibriometry*, ed. Clausen, C.-F. (Elsevier, Amsterdam).
34. Sweet, H. O. (1980) *Mouse News Lett.* **63,** 19.
35. Lim, D. J., Erway, L. C. & Clark, D. L. (1978) in *Vestibular Mechanisms in Health and Disease*, ed. (Ed.), J. D. H. (Academic Press, London), pp. 195–206.
36. Lane, P. (1986) *Mouse News Lett.* **75,** 28.
37. Seilhamer, J. J., Randall, T. L., Yamanaka, M. & Johnson, L. K. (1986) *DNA* **5,** 519–527.
38. Seilhamer, J. J., Pruzanski, W., Vadas, P., Plant, S., Miller, J. A., Kloss, J. & Johnson, L. K. (1989) *J. Biol. Chem.* **264,** 5335–5338.
39. Chen, J., Shao, C., Lazar, V., Srivastava, C. H., Lee, W. H. & Tischfield, J. A. (1997) *J. Cell. Biochem.* **64,** 369–375.
40. Chen, J., Engle, S. J., Seilhamer, J. J. & Tischfield, J. A. (1994) *J. Biol. Chem.* **269,** 23018–2324.
41. Viljoen, C. C., Botes, D. P. & Kruger, H. (1982) *Toxicon* **20,** 715–737.
42. Lind, P. & Eaker, D. (1981) *Toxicon* **19,** 11–24.
43. Kondo, K., Narita, K. & Lee, C. Y. (1978) *J. Biochem. (Tokyo)* **83,** 101–115.
44. Dijkstra, B. W., Kalk, K. H., Hol, W. G. & Drenth, J. (1981) *J. Mol. Biol.* **147,** 97–123.
45. Dijkstra, B. W., Renetseder, R., Kalk, K. H., Hol, W. G. & Drenth, J. (1983) *J. Mol. Biol.* **168,** 163–179.